



Metallurgical Investigation of a fractured low-pressure turbine rotor (LPTR) cover plate of an aeroengine

K. Raghavendra, V. Venkatesh, M. Madan, M. Sujata*, S.K. Bhaumik

Materials Science Division, National Aerospace Laboratories, Council of Scientific and Industrial Research (CSIR), Bangalore, 560017, India

ARTICLE INFO

Keywords:
Aerospace
Low-pressure turbine cover plate
Nickel-base superalloy
Press-fitted joint
Fractography
Fatigue
Design and maintenance error
Maintenance of dimensional tolerances

ABSTRACT

A twin-engine fighter aircraft met with an accident immediately after take-off and had fallen into sea. Investigation showed that the primary cause of the accident was the fracture in the low-pressure turbine rotor (LPTR) cover plate of right hand (RH) engine. Fractography study confirmed that fractures in the cover plate have originated from incipient fatigue cracks that were developed at the pin-holes meant for assembly with the turbine disc. Investigation revealed that there was deficiency in joint preparation during refitment of the cover plate onto the disc after a fault repair servicing. As a result, there was fatigue crack initiation in multiple pin-holes and the fracture in the cover plate had occurred at these pre-existing fatigue crack locations. The situation was further aggravated because of use of pins possessing hardness substantially higher than that of the cover plate. Further, study of pin-holes on the cover plate of left hand (LH) engine showed that in general, the LPTR cover plate was susceptible to fatigue failure within the prescribed service life itself. In this article, a detailed analysis of the failure that led to the aircraft accident is presented.

1. Introduction

During the last three decades, there have been significant changes in the gas turbine technology. These changes were possible because of availability of new materials and fabrication technologies, development of high temperature coatings, and improved design of cooling systems [1–5]. The thermal efficiency and power output of a gas turbine engine can be increased by raising the turbine inlet pressure ratio and temperature [5–6]. Modern aircraft gas turbines typically operate in the temperature range 1200–1500 °C to improve both thermal efficiency and power output [7–9]. However, as the turbine inlet temperature increases, the heat transferred to the engine components also increases. Therefore, if proper cooling system is not designed, the metal temperature may exceed the permissible limit for safe operation [8–9]. In gas turbine engines, the cooling air is bled from the compressor and directed towards turbine rotor and stator components, and engine casing [7,9]. The cooling of the turbine rotor and stator blades is achieved through use of hollow air-cooled blades. The turbine disc cooling is achieved by providing a cover plate which channelizes the bleed air flow over the disc surface before entering the hollow rotor blades [10–11]. The cover plate is assembled onto the disc such that it forms an integral part of the disc and hence, while in operation, the cover plate rotates at the same RPM as that of the turbine disc. During engine operation, since the cover plate along with the disc is subjected to centrifugal force and vibration, design of the attachment and fitment of the cover plate onto the disc is very critical. Any deficiency in the attachment/joint design or fitment would result in failure of either

* Corresponding author.

E-mail address: msujata@nal.res.in (M. Sujata).

the disc or the cover plate or both, and thereby jeopardising the safe operation of the engine.

Fatigue cracking is the most common cause of failure in aircraft structural components and it accounts for about 55% of total failures [12]. Fatigue failure is predominant in aircraft components because of the prevailing vibration and repetitive loading cycles. Turbine disc is one of the most critical aero-engine components and it operates under high thermal gradient and high rotational speed. While high speed results in large centrifugal force, high temperature reduces the material strength. Therefore, exceeding the operating conditions, especially, over-speeding beyond the permissible limit often leads to sudden fracture in turbine discs [13–14]. Generally, turbine discs are designed to endure 3–5% over-speed for a short duration of a few seconds. On the other hand, sustained over-speed and over-temperature results in creep deformation of the disc leading to associated failures. Other common mechanism of turbine disc failure is fatigue. The most vulnerable regions for fatigue crack initiation in turbine discs are dovetail rim region (at serrations), hub zone and the assembly holes [13]. Since the cover plate is attached to the turbine disc as an integral part, it also experiences similar mechanical and thermal loading with the vulnerability of fatigue failure as that of the disc itself.

In this article, failure of a Low Pressure Turbine Rotor (LPTR) cover plate of a gas turbine engine that led to an aircraft accident is discussed. The cover plate was made of a nickel-base superalloy and it was assembled onto the turbine disc to channelize the bleed air flow for cooling of the disc as well as the rotor blades. Detailed metallurgical investigation was carried out on the failed cover plate for identification of mode of fracture and the primary cause(s) of failure.

2. Background of the accident

There was an accident to a twin-engine fighter aircraft during a routine sortie. As reported, all the events from aircraft starting to takeoff were uneventful. Pilot noticed “Right hand (RH) engine” fire warning at 42 s after takeoff. RH engine was immediately shut down and the fire extinguisher was pressed on. Pilot continued flying maintaining attitude and direction with max dry rating on Left hand (LH) engine for about 60 s after the appearance of the first fire warning. Following this, there was total loss of control in the aircraft due to failure in the hydraulic system. Soon after, the pilot ejected and the aircraft crashed into a sea. Analysis of the black box data confirmed pilot’s account of the engine and aircraft behaviour prior to the crash. It could be established that the failure of the RH engine was indeed the cause of the aircraft accident.

2.1. Engine history

As per the records, the RH engine was subjected to repair two times since its induction into service because of oil temperature related issues. During each of these repairs, the cover plate was dis-assembled from the Low Pressure Turbine Rotor (LPTR) disc by drilling out the press-fitted pins, subjected to NDT inspection and then refitted. Total service life of the engine at the time of failure was 421:13 h and the service life since last repair was 97:00 h.

2.2. Wreckage Examination and findings

The wreckage of the aircraft was retrieved from the seabed. Examination revealed that while the LH engine suffered only minor impact damages, the RH engine was severely damaged and mangled (Fig. 1). On the left side of the RH engine, a puncture was noticed on the outer casing at 90° clock position looking from rear of the aircraft. The damages on the engine casing at the corresponding location are shown in Fig. 2. The damage pattern indicated that an object from the engine had ejected through the casing with high velocity. The impact of the ejected object was so high that it resulted in curling of the metal part at the punctured location of the casing. It was, therefore, evident that the ejected object was nothing but a part of a rotor component of the turbine and the ejection of the object occurred when the engine was in power.

Fig. 3(a) shows the damaged LPTR. The cover plate of the LPTR was found fractured and dislodged from the attachment with the LPTR disc. A part of the cover plate was found pierced into the inner casing of the engine. There were damages to all LPTR blades; seven blades were found fractured from the root region and the rest had fractured at the tip region with major damages to trailing edge (Fig. 3



Fig. 1. Damaged RH engine retrieved from the sea bed; looking from right side.



Fig. 2. Damage to the outer casing of the engine looking from left side; damage was caused due to ejection of a large object from inside the engine.

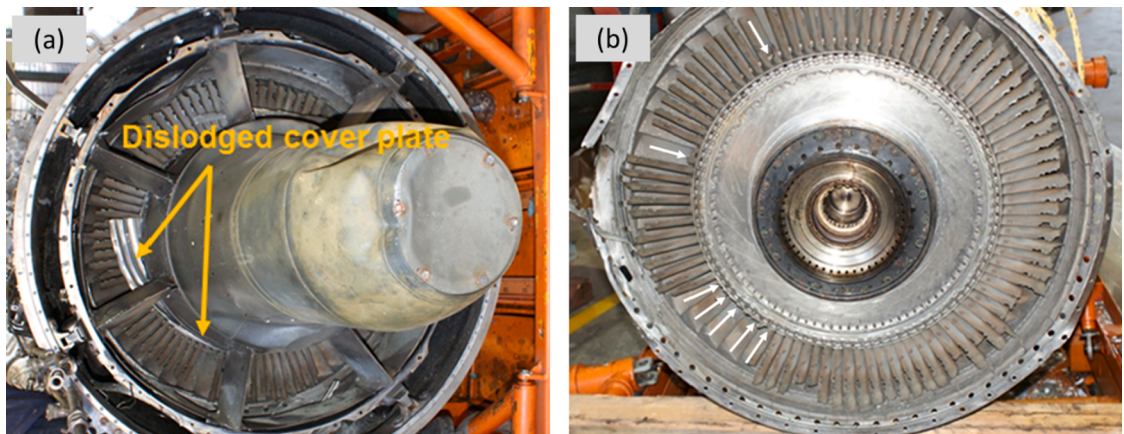


Fig. 3. Damage to the engine casings looking from left side (a) outer casing, and (b) inner casing; seven fractured blade locations are shown by arrows in (b).

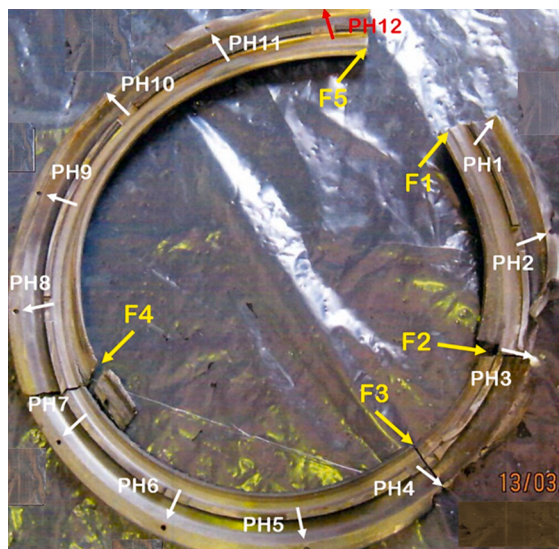


Fig. 4. Four fragments of the LPTR cover plate that were recovered; the 5th one could not be retrieved; pin-holes (PH) and fracture (F) locations are shown by arrows.

(b)).

On dis-assembly of the engine, the cover plate of the LPTR disc was found to have fractured into five pieces (Fig. 4). Out of these, four fragments were available in the engine. One fragment could not be retrieved and this piece appeared to be the first fractured part that got ejected from the engine by piercing through the casing.

2.3. Sequence of events leading to accident

Based on the physical examination of the wreckage, strip examination of the RH engine, damage patterns on the engine, damages to various engine components, and analysis of the black box data, the following sequence of events that led to the accident could be established.

- The first event in the chain of events that led to the damage to the RH engine was the fracture and dislodgement of the LPTR cover plate.
- A part of the fractured LPTR cover plate ejected through the casing under the centrifugal force. The ejection of fractured part occurred at approximately 90° clock position.
- The size of the ejected piece of the LPTR cover plate was substantially large to cause the damage of the kind seen on the engine casings. The ejected object subsequently impacted on the adjacent airframe structure leading to puncturing a hole and further damage to components mounted on the structure.
- The fragments of the engine casings, LPTR cover plate and the components outside the engine casing impacted on the pipelines of the booster and main hydraulic system causing damage/fracture.
- The fracture in the hydraulic pipelines resulted in leakage of the hydraulic oil and fire in the engine, and eventually, there was no hydraulic pressure for operation of the control surfaces.
- Subsequently, the aircraft lost total control, pilot ejected and the aircraft crashed.

2.4. Cover plate assembly

The cover plate was assembled onto the LPTR disc through bayonet type joint. There were 12 such joints equally spaced along the circumference (Fig. 4) and each joint was press fitted with a pin. While the radial movement of the cover plate was restricted by the lug on the rim of the LPTR disc, the circumferential rotation was arrested by the press fitted pins. The schematic of the joint is shown in Fig. 5. Both LPTR disc and the cover plate were made of Ni-base superalloy, and the pins were made of Fe-base superalloy.

3. Materials and methods

The fractured LPTR cover plate was examined visually and under a stereo-binocular microscope (Olympus Make, Model SZX-7). Samples containing the fracture surfaces were sectioned from the cover plate fragments and subjected to scanning electron fractography study for identification of crack origin, and the mechanism of crack propagation using a Carl Zeiss-Make Model EVO18 Scanning Electron Microscope (SEM). Microstructural studies were conducted on metallographically prepared samples using an optical microscope (Leica Make, Model DMI5000). Compositions of material of construction of the LPTR cover plate and the pins were

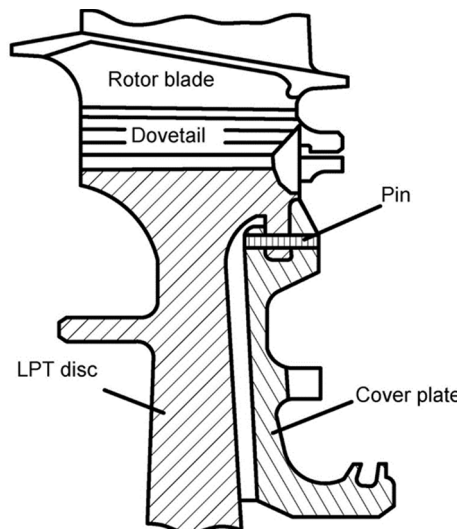


Fig. 5. Schematic showing the cover plate assembly onto the LPTR disc using the pin.

determined using an EDAX make energy dispersive X-ray (EDX) analyser attached to the SEM. Hardness measurements were conducted using a Vickers micro-hardness tester at a load of 500 g (Leica Make, Model VMHT MOT).

4. Results

4.1. Visual and stereo-binocular examination

The LPTR cover plate was found to have five fractures, marked F1 through F5 in Fig. 4. The locations of the pin-holes (PHs) meant for fitment of cover plate on to LPTR disc have also been marked in the figure. Examination revealed that three of the fractures, namely, F1, F2 and F3 were along the pin-holes PH1, PH3 and PH4 respectively. The remaining two fractures (F4 and F5) were away from pin-holes location.

The fragment of the LPTR cover plate between the fractures F1 and F5 (designated as fragment (FRG) 1) had ejected first from the engine by piercing through the casing and this fragment could not be retrieved from the wreckage. Examination of the fractured parts of the LPTR cover plate revealed that the FRG-2 and FRG-3 suffered severe post-fracture damages, while FRG-5 was partially damaged. The fragment designated as FRG-4 was largely undamaged except for minor fracture close to PH4. Out of the 12 pins used for assembly of cover plate on to the LPTR disc, only two fractured pins were available at locations PH5 and PH12, and the rest were unavailable.

4.2. Study of fracture surfaces of the cover plate

All the fracture surfaces of the LPTR cover plate fragments were found severely damaged. Fracture features at and around PH1 were obliterated due to post fracture damages, associated with both mechanical damages and corrosion effects (Fig. 6). Similar observations were made on the fracture along PH3 and PH4 as well. Some of the fracture surfaces showed presence of chevron marks away from the crack initiation regions while the others were found to be covered with a thick layer of oxidation/corrosion products (Fig. 7(a)). Away from pin-holes, in regions where the fracture surface was relatively preserved, crack propagation was found to be by intergranular mode, typical of overload failure in Ni-base superalloy components at elevated temperatures (Fig. 7(b)).

Two fractured pins that were available with the segments of the LPTR cover plate showed gross features typical of overload failure. The fracture was associated with deformation in the pins. The fracture surface was covered with a thick and firmly adherent layer of corrosion products and hence, micro-fracture features were not discernible (Fig. 8).

4.3. Incipient cracks at pin-holes

Examination revealed presence of incipient cracks in five pin-holes out of the remaining nine pin-hole surfaces where there was no fracture. These are at PH2, PH5, PH6, PH7 and PH8. In each of these pin-holes, two incipient cracks were found located at diametrically opposite locations and oriented in the radial direction of the cover plate. The appearance of these cracks in two typical pin-holes are shown in Figs. 9–10. Cracks in two arbitrarily chosen pin-holes were pulled open for further study and the resulting fracture surfaces are shown in Fig. 11. The crack surfaces showed presence of a discoloured region with a quarter-circular shape, typically observed in the case of progressive crack propagation. In this region, although the fracture features were largely obliterated due to oxidation and corrosion, some regions on the surface were found relatively preserved. Examination of these regions, after repeated replica cleaning, showed presence of well-delineated striations, typical of fatigue crack propagation (Figs. 12–13). The orientation of the striations suggested that the fatigue crack had initiated at the pin-hole edge on the LPTR cover plate. The depth of the fatigue cracks was measured to be in the range 0.5–0.8 mm.

Fig. 14(a) shows the SE image of metallographically prepared surface of PH5. Magnified views of the two incipient cracks emanating from the pin-hole edge are shown in Fig. 14(b–c). Fig. 14(d) shows the nature of crack propagation in the bulk of the material. The crack propagation was found to be predominantly by transgranular mode.

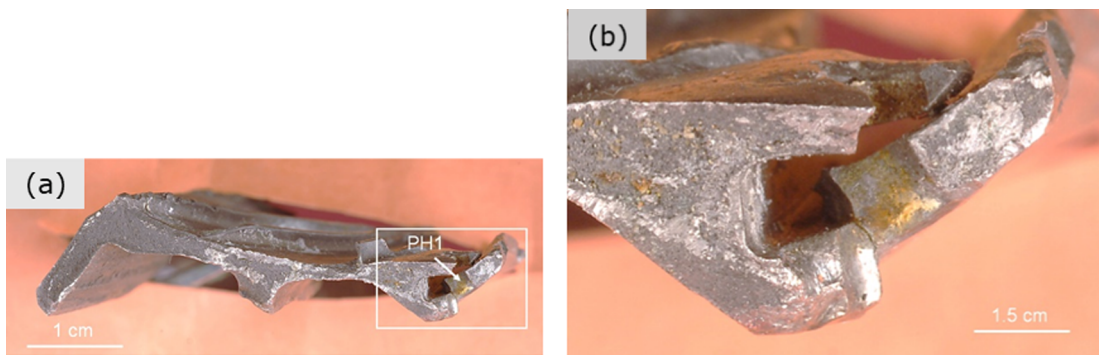


Fig. 6. (a) Fracture surface of the LPTR cover plate marked F1 in Fig. 4, and (b) magnified view of the region marked in (a) showing fracture surface of PH1.

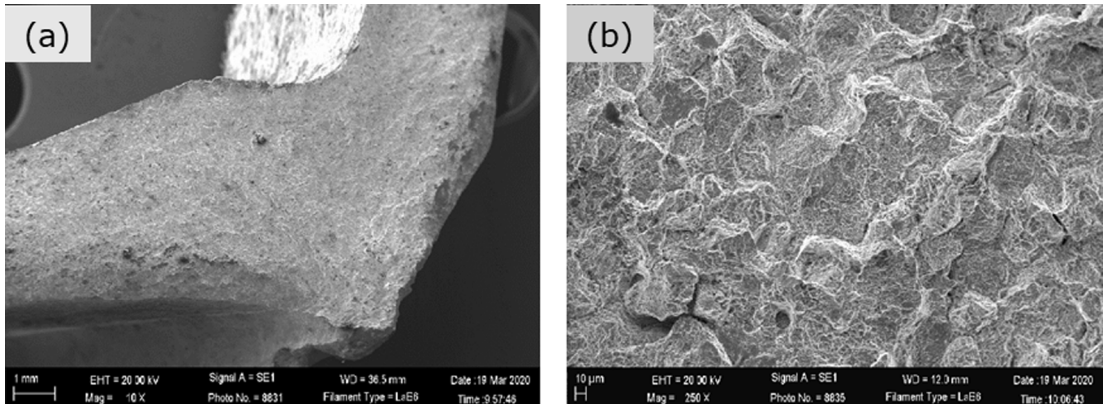


Fig. 7. (a) Secondary electron (SE) fractograph of a typical region on the fracture surface in Fig. 6 showing chevron marks emanating from an edge, and (b) intergranular fracture features at high magnification.

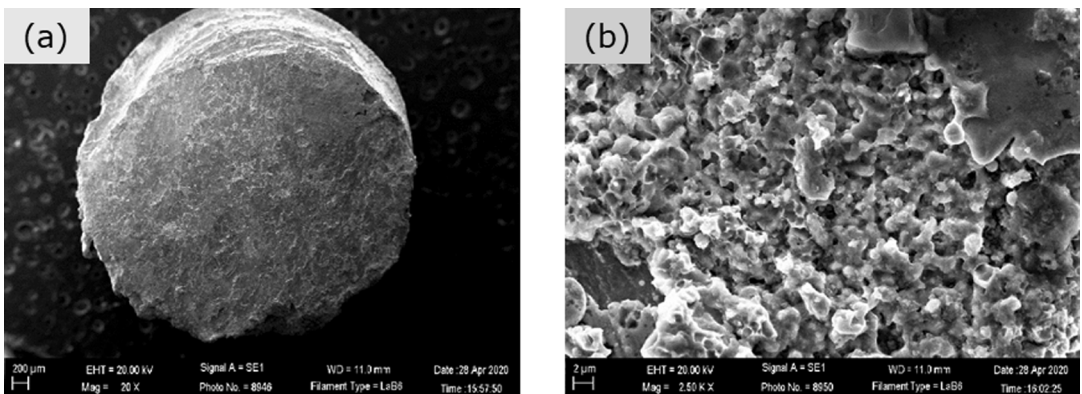


Fig. 8. Secondary electron (SE) images from (a) fracture surface of one of the two fractured pins that were available with the segments of LPTR cover plate, and (b) thick layer of corrosion products on the fracture surface shown in (a).

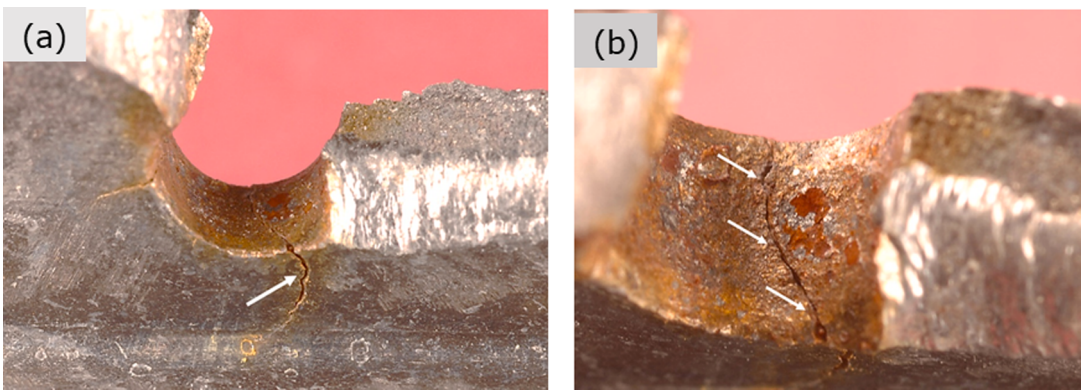


Fig. 9. A propagating crack in PH2, (a) on the rear face of the cover plate, and (b) on the pin-hole surface.

4.4. Fitment of cover plate with LPTR disc

Fig. 15 shows the PH12 on the LPTR cover plate with the pin in position. Examination revealed that while the pin had a circular cross section with a close tolerance on diameter in the range 3.96–3.99 mm, the pin-hole on the cover plate had oval shape with dimensions of 4.24 and 3.99 mm respectively at two perpendicular directions (Fig. 15, Table 1).

Fig. 16 shows the microstructure of the LPTR cover plate material at the peripheral region of the pin-hole at two different regions.

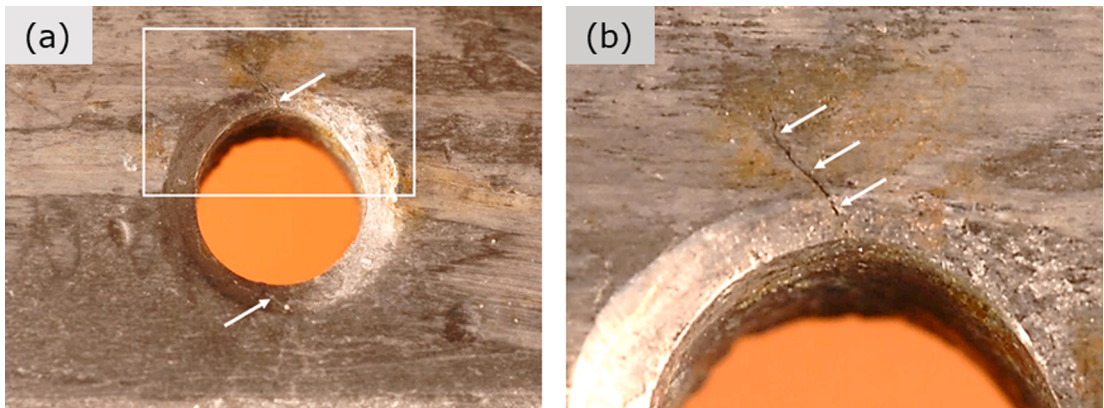


Fig. 10. (a) Two propagating cracks emanating from PH6 in the radial direction, and (b) magnified view of the crack marked in (a).

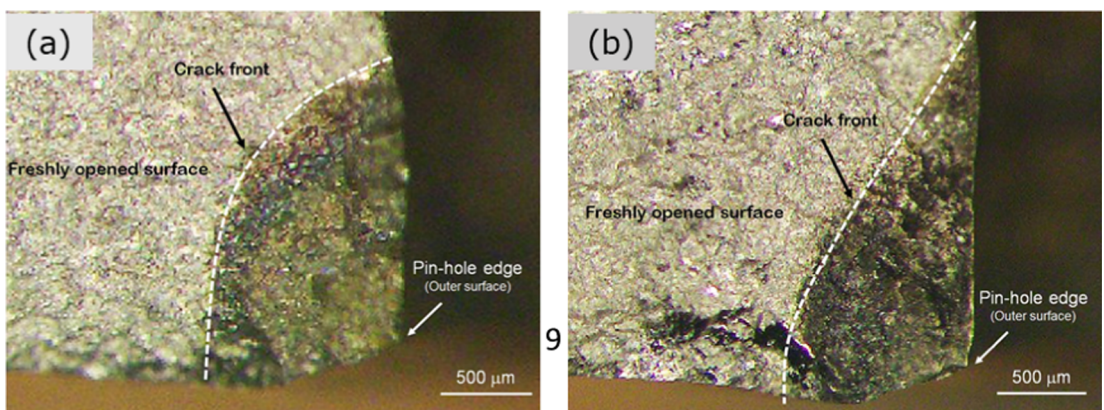


Fig. 11. Appearance of the crack surfaces after being pulled open (a) PH6, and (b) PH7.

These two regions correspond to location where there was no contact with the pin (Fig. 16(a)), and location where there was contact with the pin (Fig. 16(b)). In both the regions, the microstructure was found to consist equiaxed grains with no evidences of deformation, thereby, ruling out the possibility of pin-hole undergoing deformation during service or during the process of fracture of the pin.

4.5. Material of construction

4.5.1. Chemical composition

The composition of the LPTR cover plate and the pin materials was determined by energy dispersive X-ray (EDX) analyser attached to SEM. Results showed that the cover plate was made of Ni-base superalloy, and the pins were made of an iron-base superalloy (Tables 2-3). The material of construction of both the components was found to conform to their respective specifications.

4.5.2. Microstructure

Fig. 17 shows the microstructures of the LPTR cover plate. The material possessed a microstructure consisting of polycrystalline Ni-rich γ -matrix phase dispersed with γ' -precipitates, and carbide particles at grain boundaries. Fig. 18 shows the microstructure of the assembly pins of the cover plate. The microstructure consisted of polycrystalline austenite grains and uniformly distributed carbide particles. There were no deleterious phases in the microstructure of either the cover plate, or the pins. Also, there were no evidences of temperature assisted deterioration in the material of construction.

4.5.3. Hardness

Hardness of the material of the LPTR cover plate and the pin was measured on metallographically prepared samples using a Vickers hardness tester at a load of 500 g. The average hardness of the LPTR cover plate and pin was measured to be 416 and 496 HV_{0.5} respectively (Fig. 19).

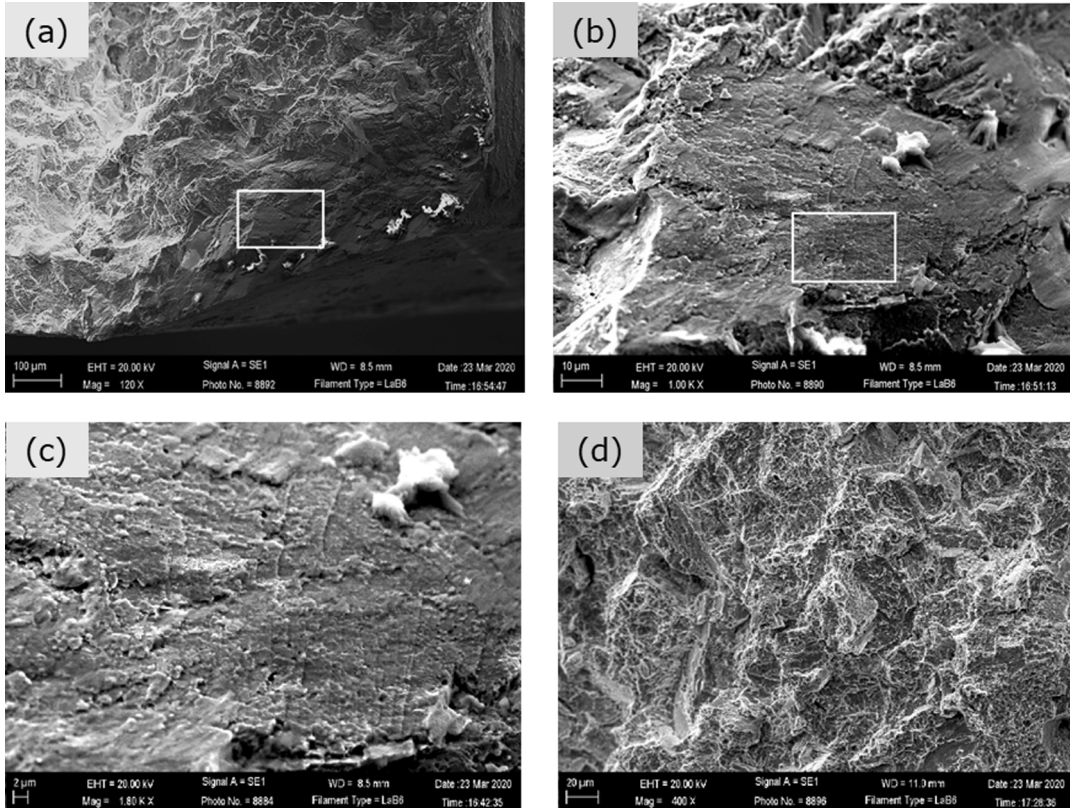


Fig. 12. SE fractographs from (a) crack surface shown in Fig. 11(a), (b) and (c) magnified views of the regions marked in (a) and (b) respectively showing fatigue striations, and (d) dimple rupture on the freshly opened surface.

4.6. Examination of L PTR cover plate of LH engine

In view of initiation of fatigue cracks at several pin-holes of the L PTR cover plate of RH engine, investigation was conducted on the joints of another serviceable cover plate to examine for distress, present, if any. For this study, the cover plate of LH engine was chosen since the LH engine had a service life of 420:20 h, similar to that of the RH engine (421:13 h). As per records, the LH engine was not subjected to any repair or overhaul since new. The cover plate with the L PTR disc of the LH engine used for the investigation is shown in Fig. 20. The central portion of the disc was machined out for ease of handling during laboratory studies.

4.6.1. Fitment of cover plate with L PTR disc

All the 12 press fitted joints on the cover plate were examined under a stereo-binocular microscope. None of the pin-holes on the cover plate was found to have developed cracks. Two samples containing the press fit joints were sectioned by Electro Discharge Machining (EDM) from approximately diametrically opposite locations on the cover plate, metallographically prepared and examined under a scanning electron microscope. Cross sectional views of these joints are shown in Fig. 21. The fitment in both the joints was found to be satisfactory and the dimensions of the pins and the pin-holes were found to be within the tolerances (Table 1).

4.6.2. Pin-hole surfaces

Pin-hole surfaces of two of the randomly selected joints were exposed after sectioning by EDM for further examination as shown in Fig. 22. Under the SEM, coarse slip bands were observed on the pin-hole surfaces (Fig. 23). The slip bands were found to be oriented along the longitudinal direction of the pin-holes. In a few places, initiation of cracks along the slip bands was also observed and a typical one is shown in Fig. 23(d). For further confirmation, marginal tensile load was applied on the pin-hole surfaces. Application of tensile load resulted in widening of the existing cracks and generation of enumerable number of cracks along the slip bands (Fig. 24).

5. Discussion

The outcome of the fractography study on the existing fracture surfaces of the L PTR cover plate of RH engine was not very conclusive because of the obliteration of the fracture features at the crack origin regions due to post-fracture mechanical damage and/or oxidation and/or corrosion. Examination, however, showed presence of incipient cracks emanating from five pin-holes on the fractured L PTR cover plate segments. All these crack surfaces showed presence of well-delineated striations, indicative of crack

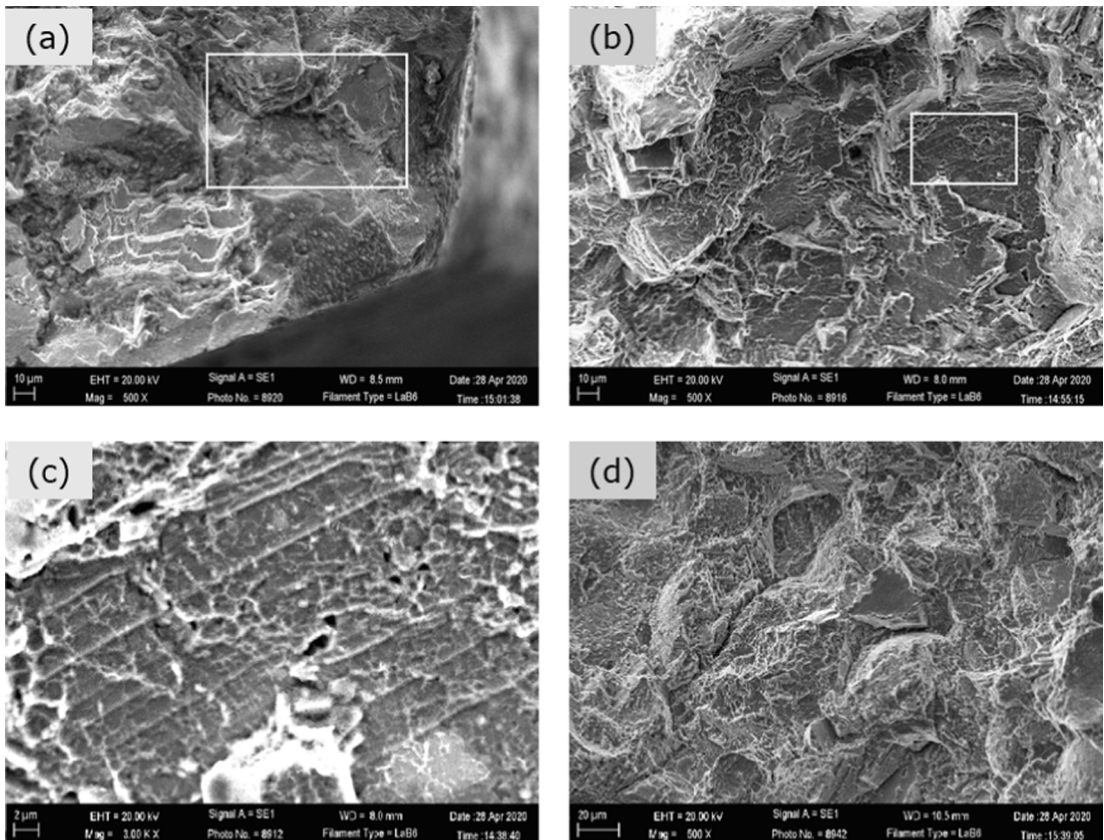


Fig. 13. SE fractographs from (a) crack surface shown in Fig. 11(b), (b) and (c) magnified views of the regions marked in (a) and (b) respectively showing fatigue striations, and (d) dimple rupture on the freshly opened surface.

initiation and propagation by fatigue mechanism. The orientation of the striations indicated that the fatigue cracks had initiated at the edge of the pin-holes. In view of this, inference could be drawn that the major/main fractures in the LPTR cover plate had originated from these incipient fatigue cracks at the pin-holes, which in turn, were responsible for the failure of the RH engine leading to the accident.

Investigation revealed deficiency in the fitment of the LPTR cover plate with the LPTR disc wherein there was improper joint preparation during refitment after repair. It was found that although the pin had a circular cross section with close tolerances, the pin-hole on the cover plate was not circular and had an oval shape. As a result, the contact between the pins and the hole-surfaces on the cover plate was limited to localized regions. Since the hardness of the pin was higher than that of the cover plate, while press fitting, the cover plate material at the contact regions of the pin-holes was under compression leading to generation of tensile stresses along the periphery of the hole at the non-contact regions. The magnitude of tensile stresses generated would depend on the tolerances between the hole and the pin dimensions, and it would vary from one joint to the other. In pin-holes, where the tensile stresses were at the threshold limit, fatigue cracks had initiated from the edge of the holes and propagated preferentially in the radial direction of the cover plate. Study revealed that the reworking/refitment scheme adopted on the cover plate was not a foolproof method for ensuring the profile and dimensional requirements of the pin-holes.

In press-fitted joints, the hardness of the pin material is generally maintained lower than that of the components being joined together. Lower hardness of pin ensures uniform contact of the pin over the entire pin-hole surface during press fitting. From the manufacturing point of view, this also allows certain margin on the tolerances of the pin and pin-hole in terms of ovality [15]. In the present case, however, the hardness of the assembly pin was higher than that of the cover plate by about 80 units on HV_{0.5} scale. Analysis suggested that this was also a contributory factor for the failure of the cover plate.

L PTR disc and the cover plate are subjected to low-cycle fatigue (LCF) during start-up, normal operation and shut-down of the engine. During LCF loading, plastic deformation in Ni-based superalloys leads to formation of slip bands [16]. In each LCF cycle, dislocations multiply and accumulate within the material resulting in increase in their density. These dislocations arrange themselves in low energy configurations resulting in formation of persistent slip bands (PSB). PSBs are formed due to cyclic intrusion and extrusion. Coarse surface slip bands have hill-and-valley topography resulting from this cyclic intrusion and extrusion. As a result, surface relief is formed by cyclic plastic deformation first and then, the cracks initiate at the roots of the built-up surface intrusions, that is, at the surface micro-notches. PSBs are the precursors to fatigue crack initiation [13,16–17].

Development of extensive PSBs on the pin-hole surfaces of the LH engine cover plate and generation of cracks at some of these PSBs

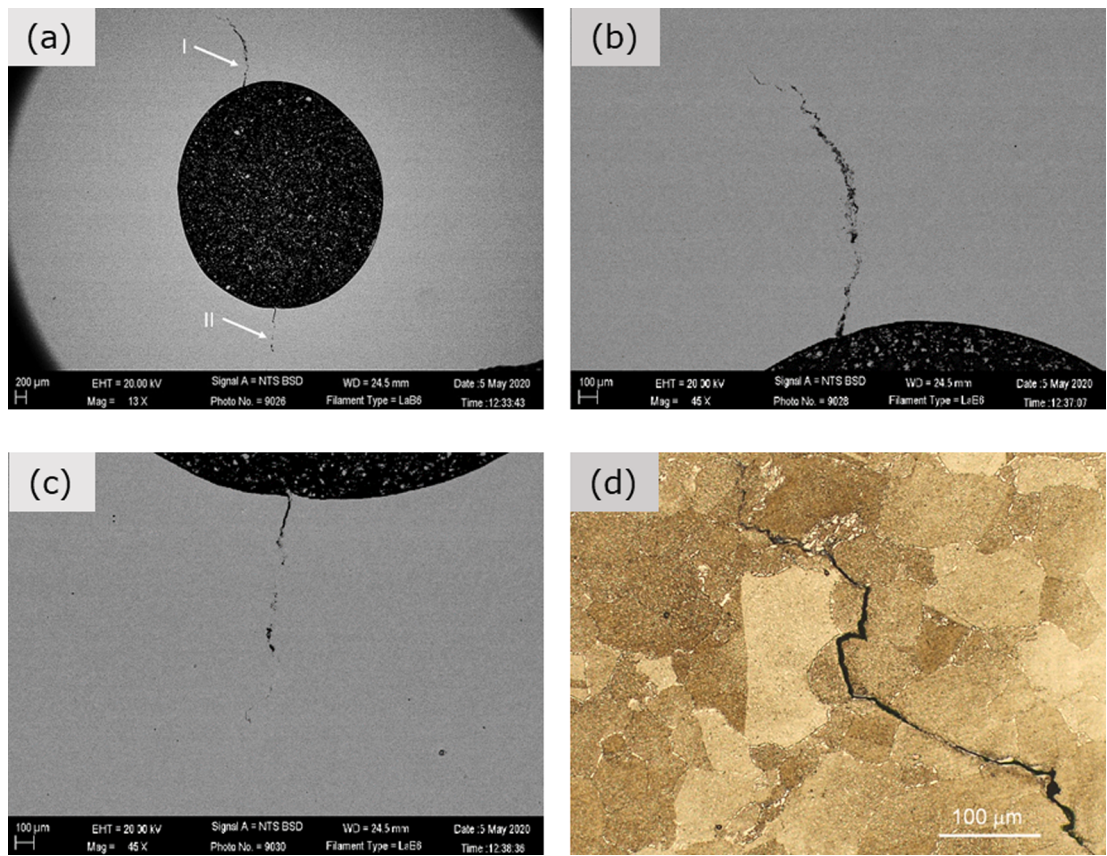


Fig. 14. (a) SE image of metallographically prepared PH8 surface showing cracks emanating from the hole, (b-c) close-up views of the cracks, and (d) optical micrograph at the tip of the crack in (b) showing transgranular mode of crack propagation.

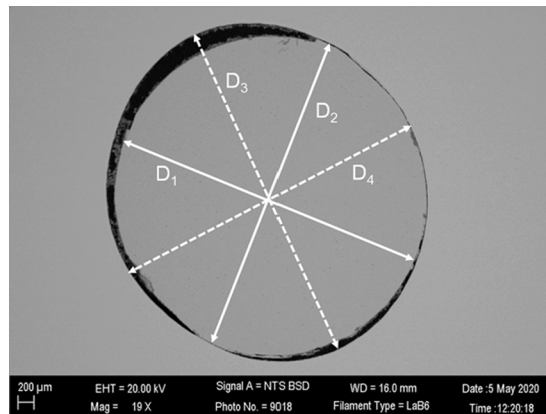


Fig. 15. SE image of metallographically prepared surface of PH5 showing pin and pin-hole profiles (D₁, D₂: pin dimension; D₃, D₄: pin-hole dimension).

indicated that the fatigue damage around the pin-holes has already reached the threshold limit for initiation and propagation of fatigue cracks. Since RH engine had identical service life (~420 h) as that of the LH engine (~421 h), similar fatigue damage would have occurred around the pin-holes of the LPTR cover plate of RH engine as well. Theoretical and experimental studies have established that fatigue cracks in structural components reduce the tensile fracture strength significantly [18]. In some cases, reductions in fracture strength up to 50% have been reported [19]. Therefore, under LCF loading conditions, generation of small fatigue cracks even of the order of a few hundreds of microns can result in sudden fracture in the components. The LPTR cover plate in question is subjected to high centrifugal forces and vibrations that are transferred to the disc through the joints. Therefore, presence of fatigue cracks on the

Table 1

Dimensions of pin and pin-holes on the cover plates of LH and RH engines; measured at two perpendicular directions.

| Engine ID | Pin dimension (μm) | | Pin-hole dimension (μm) | |
|----------------------|---------------------------------|-------|--------------------------------------|-------|
| | D_1 | D_2 | D_3 | D_4 |
| RH engine (Fig. 15) | 3990 | 3960 | 4240 | 3990 |
| LH engine | | | | |
| Joint 1 (Fig. 21(a)) | 3922 | 3936 | 3943 | 3968 |
| Joint 2 (Fig. 21(b)) | 3923 | 3929 | 3993 | 3957 |

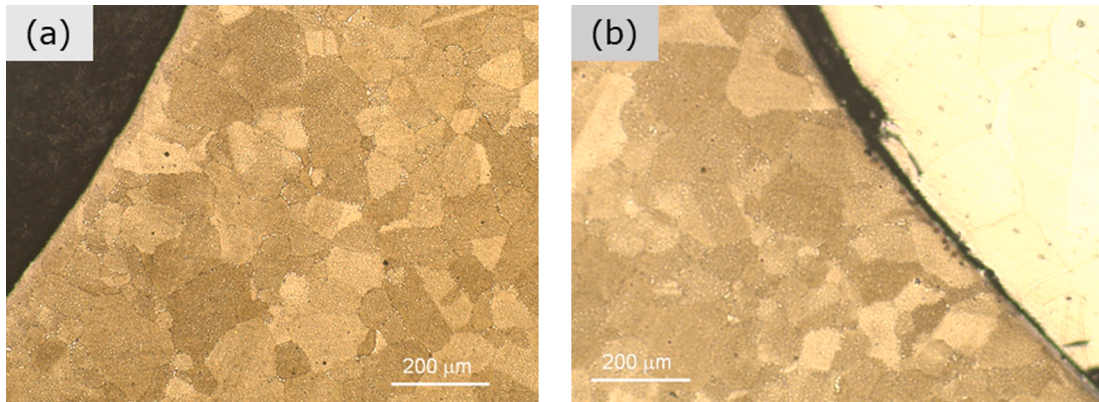


Fig. 16. Optical micrographs showing no deformation in the cover plate material at the pin-hole periphery (PH5): (a) region with no contact with the pin, and (b) region in contact with the pin.

Table 2

Semi-quantitative composition analysis of the material of construction of the L PTR cover plate; carried out using EDX analyzer *.

| Elements | Composition (wt.%) L PTR cover plate | Specification |
|----------|---|---------------|
| C | * | 0.06 |
| Al | 6.1 | 5.1 – 6.2 |
| Nb | 2.2 | 1.8 – 2.8 |
| Mo | 3.0 | 2.5 – 3.7 |
| Ti | 2.2 | 1.8 – 2.9 |
| Cr | 9.8 | 9.5 – 11.5 |
| Mn | 0.5 | 1.0 max |
| Co | 15.6 | 14.4 – 16.4 |
| Ni | 56.1 | Balance |
| W | 4.5 | 3.8 – 5.2 |

* Carbon cannot be determined accurately by EDX analysis.

pin-hole surfaces would make the cover plate vulnerable to catastrophic fracture, especially during start-up and shut-down of the engine.

Despite satisfactory fitment of the L PTR cover plate in LH engine, formation of extensive PSBs on the pin-hole surfaces and initiation of fatigue cracks at these PSBs points towards inadequacy in the design of the cover plate assembly with the disc. It is evident that the cover plate did not have the safe fatigue life under the prevailing operating conditions. In case of cover plate of the RH engine, improper joint preparation during the last repair and the use of pin with high hardness had aggravated the situation further in accelerating the failure.

6. Conclusions

In this study, failure of a L PTR cover plate of an aero-engine has been investigated. The fracture in the cover plate was responsible for the engine failure leading to the accident to the aircraft. Fractography study showed that the failure in the cover plate was by fatigue mechanism. Investigation revealed that the premature failure in the cover plate occurred due to combination of multiple factors and these are as follows.

Table 3

Semi-quantitative composition analysis of the material of construction of the assembly pins of the LPTR cover plate; carried out by EDX analyzer *.

| Element | Composition, wt.% | Specification |
|---------|-------------------|---------------|
| | Pin material | |
| C | * | 0.08 |
| Mn | 0.4 | 2.0 max |
| Si | 0.8 | 1.0 max |
| Cr | 14.2 | 13.5 – 16.0 |
| Ni | 25.7 | 24.0 – 27.0 |
| Mo | 1.1 | 1.0 – 1.5 |
| Ti | 2.3 | 1.9 – 2.35 |
| V | – | 0.1 – 0.5 |
| Al | – | 0.35 max |
| Co | – | 1.0 max |
| Cu | – | 0.5 max |
| Fe | Balance | Balance |

* Carbon cannot be determined accurately by EDX analysis.

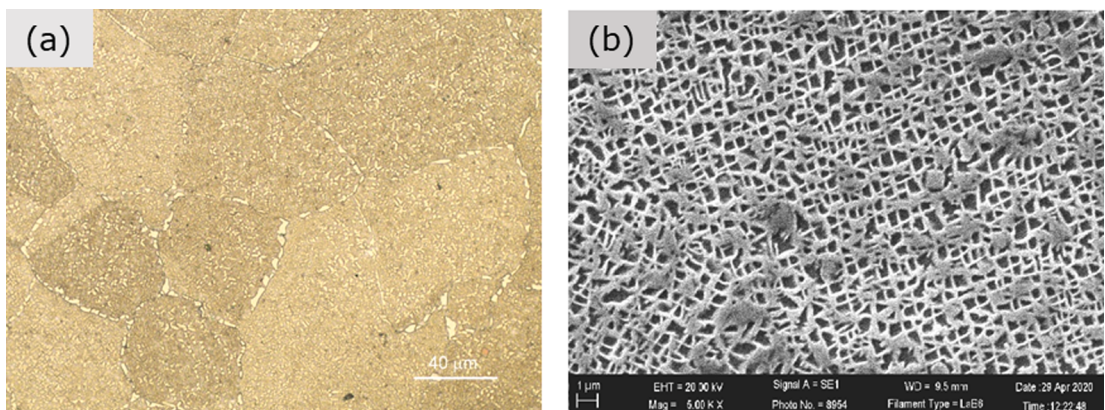


Fig. 17. Microstructure of the LPTR cover plate material consisting of Ni-rich γ -matrix dispersed with γ' -precipitates and carbide particles: (a) optical, and (b) secondary electron micrographs.

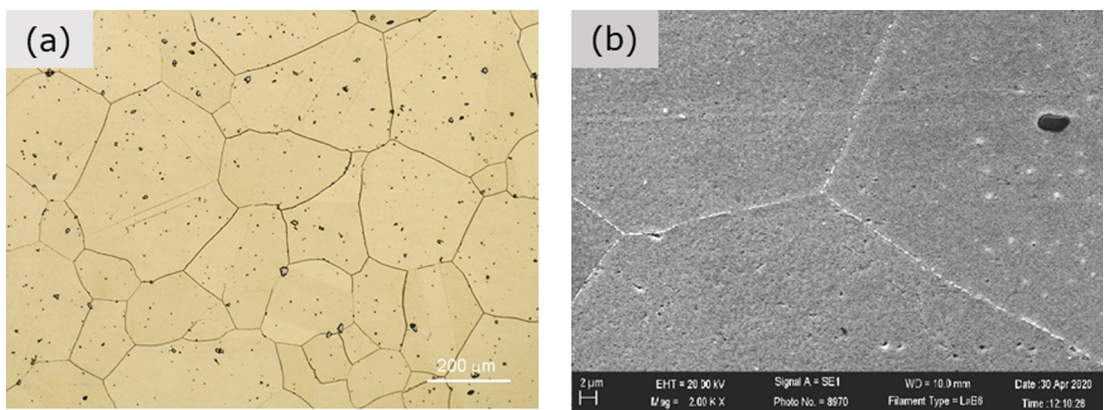


Fig. 18. Microstructure of the material of construction of the pin in PH5 consisting of polycrystalline austenite grains and uniformly distributed carbides: (a) optical and (b) secondary electron micrographs.

- (a) There was inadequacy in the design of the cover plate assembly with the disc, and hence, it did not have safe fatigue life under the prevailing operating conditions.
- (b) The cover plate failure was accelerated due to improper joint preparation during the last repair of the engine wherein the tolerances on the ovality of pin-holes were not maintained.
- (c) The use of pins with hardness substantially higher than that of the cover plate was another factor that contributed to the failure.

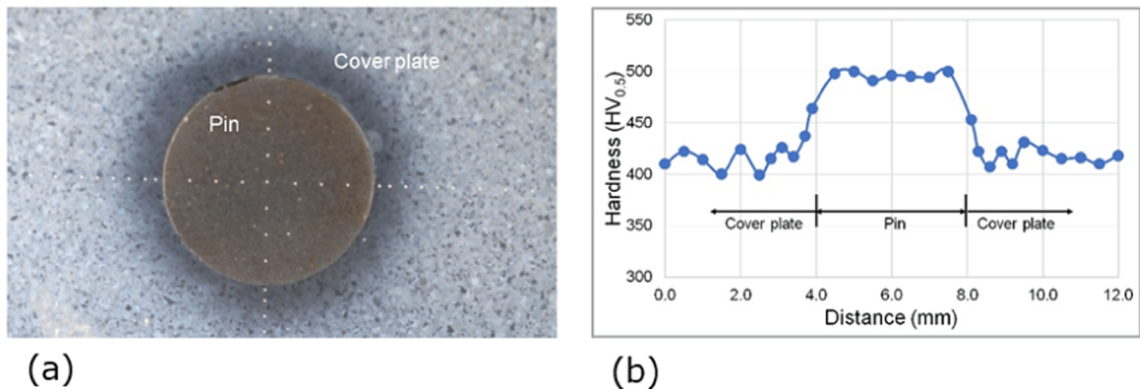


Fig. 19. (a) Metallographically prepared pin in PH12 for hardness survey, and (b) hardness vs distance plot.

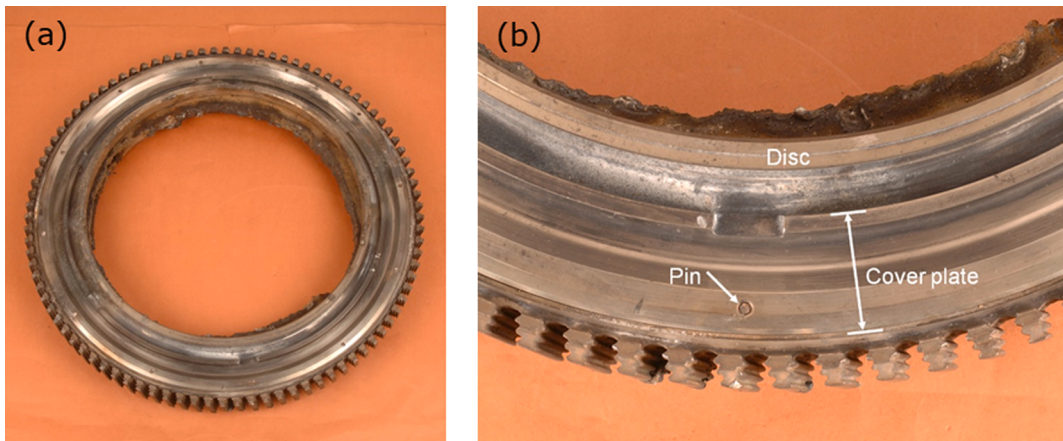


Fig. 20. (a) L PTR disc of LH engine along with the cover plate in position (central portion of the disc was removed for ease of handling in the laboratory), and (b) close-up view showing cover plate, assembly pin and L PTR disc.

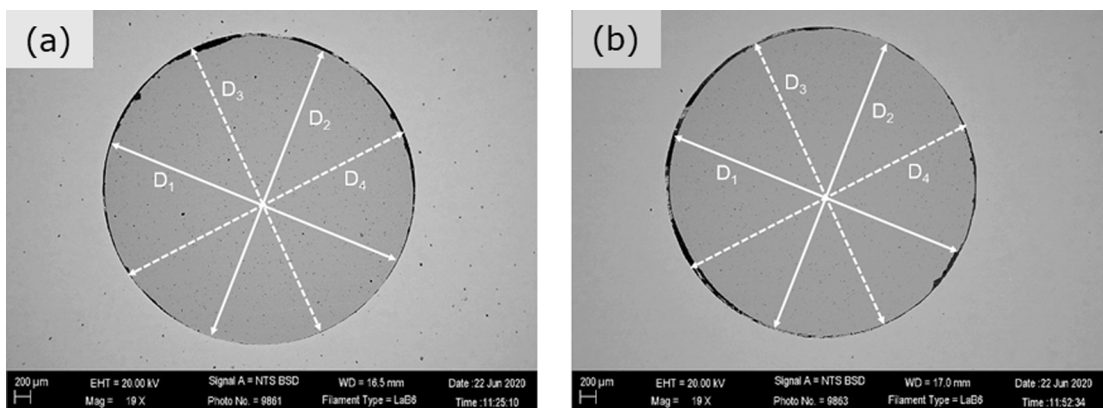


Fig. 21. SE images of metallographically prepared joints of L PTR cover plate of LH engine showing pin and pin-hole profiles: (a) joint 1, and (b) joint 2 (D₁, D₂: pin dimension; D₃, D₄: pin-hole dimension).

7. Preventive actions

- (a) Tolerances as per the design specification should be maintained between the pin and the pin-hole to ensure satisfactory press-fit joint.

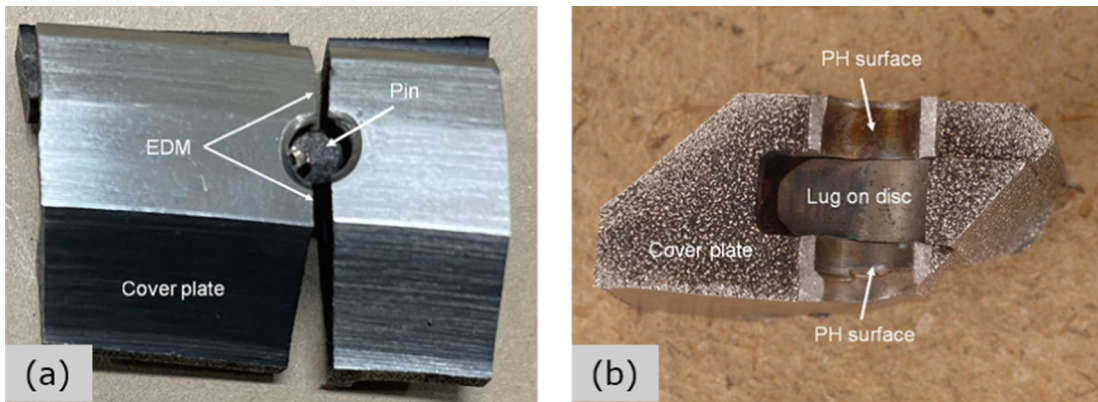


Fig. 22. (a) Sectioning of cover plate by EDM for exposing the pin-hole surface, and (b) pin-hole surface after sectioning.

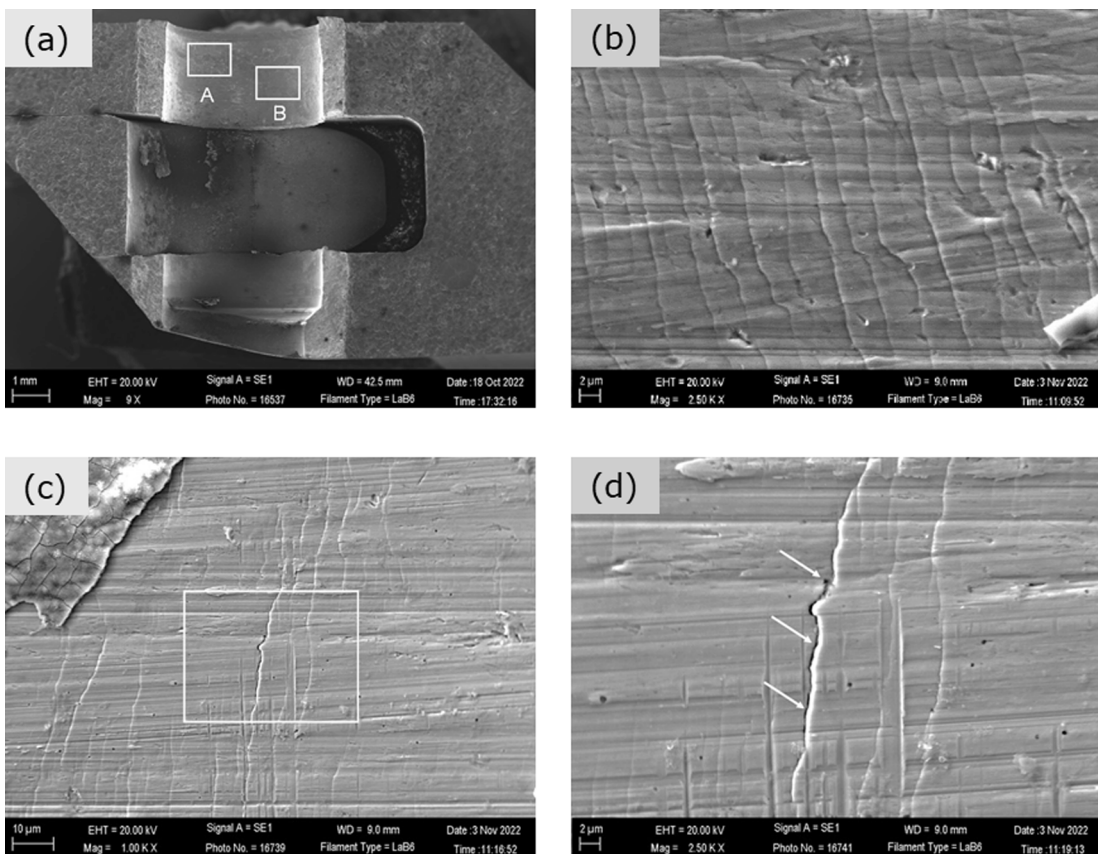


Fig. 23. (a) SE image of a typical pin-hole surface on the LPTR cover plate of LH engine, (b-c) magnified views of the regions marked 'A' and 'B' respectively in (a) showing slip bands oriented in the longitudinal direction, and (d) magnified view of a crack along a slip band marked in (c).

- (b) Removal of the cover plate from the LPTR disc by drilling out the pins is likely to alter the profile of the pin-holes on the cover plate as seen in the present case. Hence, circularity of the pin-holes within the tolerances needs to be ensured after the removal of the pins and prior to refitting the cover plate with the LPTR disc.
- (c) It is recommended to use pins with hardness lower than that of the cover plate.

Declaration of Competing Interest

The authors declare that they have no known competing financial interests or personal relationships that could have appeared to

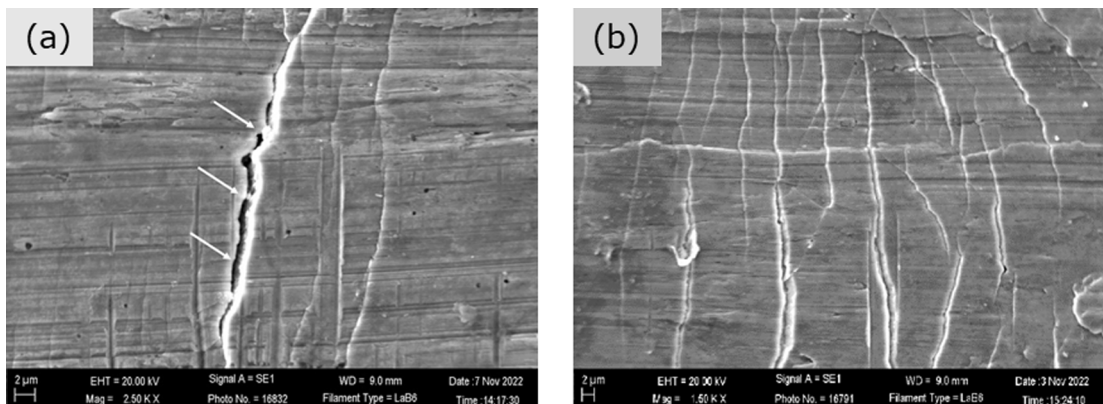


Fig. 24. SE images showing opening/widening of cracks along the slip bands after application of marginal tensile load on the pin-hole surface: (a) the crack shown in Fig. 23(d), and (b) elsewhere on the pin-hole surface.

influence the work reported in this paper.

Data availability

The data that has been used is confidential.

Acknowledgements

The authors thank the members of the investigating committee and the manufacturer for providing necessary information as and when required during the laboratory investigation of the LPTR cover plate failure. The work was financially supported by CSIR-National Aerospace Laboratories, Bangalore (Project No. M-1-298).

References

- [1] V. Yang, A review of cooling technologies for high temperature rotating components in gas turbine, Umesh Unnikrishnan, *Propuls. Power Res.* 11 (2022) 293–310.
- [2] I.G. Wright, T.B. Gibbons, Recent developments in gas turbine materials and technology and their implications for syngas firing, *Int. J. Hydrot. Energy* 32 (2007) 3610–3621.
- [3] M. Konter, M. Thumann, Materials and manufacturing of advanced industrial gas turbine components, *J. Mater. Process. Technol.* 117 (2001) 386–390.
- [4] D.R. Clarke, M. Oechsner, N.P. Padture, Thermal-barrier coatings for more efficient gas-turbine engines, *Mater. Res. Bull.* 37 (2012) 891–899.
- [5] Z. Huda, T. Zaharinie, H.A. Al-Ansary, Enhancing power output and profitability through energy-efficiency techniques and advanced materials in today's industrial gas turbines, *Int. J. Mech. Mater. Eng.* 9 (2014) 1–12.
- [6] B. Salim, J. Orfi, S.S. Alaqel, Effect of turbine and compressor inlet temperatures and air bleeding on the comparative performance of simple and combined gas turbine unit, *Eur. J. Eng. Sci., Tech.* 5 (2020) 39–45.
- [7] Luai M. Al-Hadrami, S.M. Shaahid and Ali A. Al-Mubarak, Jet impingement cooling in gas turbines for improving thermal efficiency and power density, In: "Advances in Gas Turbine Technology," Edited by Ernesto Benini, Published by InTech, Croatia, (2011) 191–210 (ISBN: 978-953-307-611-9).
- [8] R.S. Amano, *Advances in gas turbine blade cooling technology*, WIT Trans. Eng. Sci. 61 (2008) 149–157.
- [9] University of Wisconsin-Milwaukee, USA, The Jet Engine, Rolls-Royce plc, United Kingdom, 5th edition (1996), (ISBN: 0902121 235).
- [10] J.M. Owen, Air-cooled gas-turbine discs: a review of recent research, *Int. J. Heat Fluid Flow* 9 (1988) 354–365.
- [11] R. Dilip, Ballal and Joseph Zelina, Progress in aeroengining technology (1939–2003), *J. Aircr.* 41 (2004) 43–50.
- [12] S.J. Findlay, N.D. Harrison, Why aircraft fail, *Mater. Today* 5 (2002) 18–25.
- [13] L. Witek, Failure analysis of turbine disc of an aero engine, *Eng. Fail. Anal.* 13 (2006) 9–17.
- [14] I. Eryilmaz, V. Pachidis, A design approach for controlled blade-off in overspeeding turbines, *Eng. Fail. Anal.* 138 (2022), 106323.
- [15] S.K. Bhattacharjee, M. Sujata, M.A. Venkatasamy, Fatigue failure of aircraft components, *Eng. Fail. Anal.* 15 (2008) 675–694.
- [16] F.D. Leon-Cazaress, R. Schlutter, T. Jackson, E.I. Galindo-Nava, C.M.F. Rae, A multiscale study on the morphology and evolution of slip bands in a nickel-based superalloy during low cycle fatigue, *Acta Mater.* 182 (2020) 47–59.
- [17] P. Lukas, L. Kunz, Role of persistent slip bands in fatigue, *Philos. Mag.* 84 (2004) 317–330.
- [18] S. Suresh, *Fatigue of Materials*, 2nd ed., Cambridge University Press, 1998.
- [19] D. Broek, *The practical use of fracture mechanics*, Springer Science & Business Media, 2012.